



## Research article

# Integrating p53-associated genes and infiltrating immune cell characterization as a prognostic biomarker in multiple myeloma

Jun-Ting Lv<sup>a,1</sup>, Yu-Tian Jiao<sup>b,1</sup>, Xin-Le Han<sup>c,1</sup>, Yang-Jia Cao<sup>d</sup>, Xu-Kun Lv<sup>b</sup>,  
Jun Du<sup>e,f,\*\*,1</sup>, Jian Hou<sup>e,\*,1</sup>

<sup>a</sup> Zhuhai Hospital of Integrated Traditional Chinese & Western Medicine, 519000, China

<sup>b</sup> Department of Clinical Medicine, Shanghai Jiao Tong University School of Medicine, Shanghai, 200025, China

<sup>c</sup> Department of Pathology, Ninth People's Hospital, Shanghai Jiao Tong University School of Medicine, Shanghai, 200011, China

<sup>d</sup> Department of Hematology, The First Affiliated Hospital of Xi'an Jiao Tong University, Xi'an, 710061, China

<sup>e</sup> Department of Hematology, Renji Hospital, School of Medicine, Shanghai Jiao Tong University, Shanghai, 200127, China

<sup>f</sup> Department of Hematology, Punan Hospital, Pudong New District, Shanghai, 200011, China

## ARTICLE INFO

## Keywords:

Multiple myeloma (MM)  
Stratification model  
p53 signaling pathway  
Immune microenvironment  
Immune checkpoints

## ABSTRACT

**Background:** Tumor genetic anomalies and immune dysregulation are pivotal in the progression of multiple myeloma (MM). Accurate patient stratification is essential for effective MM management, yet current models fail to comprehensively incorporate both molecular and immune profiles.

**Methods:** We examined 776 samples from the MMRF CoMMpass database, employing univariate regression with LASSO and CIBERSORT algorithms to identify 15 p53-related genes and six immune cells with prognostic significance in MM. A p53-TIC (tumor-infiltrating immune cells) classifier was constructed by calculating scores using the bootstrap-multicox method, which was further validated externally (GSE136337) and through ten-fold internal cross-validation for its predictive reliability and robustness.

**Results:** The p53-TIC classifier demonstrated excellent performance in predicting the prognosis in MM. Specifically, patients in the p53<sup>low</sup>/TIC<sup>high</sup> subgroup had the most favorable prognosis and the lowest tumor mutational burden (TMB). Conversely, those in the p53<sup>high</sup>/TIC<sup>low</sup> subgroup, with the least favorable prognosis and the highest TMB, were predicted to have the best anti-PD1 and anti-CTLA4 response rate (40%), which can be explained by their higher expression of PD1 and CTLA4. The three-year area under the curve (AUC) was 0.80 in the total sample.

**Conclusions:** Our study highlights the potential of an integrated analysis of p53-associated genes and TIC in predicting prognosis and aiding clinical decision-making in MM patients. This finding underscores the significance of comprehending the intricate interplay between genetic abnormalities and immune dysfunction in MM. Further research into this area may lead to the development of more effective treatment strategies.

\* Corresponding author. Department of Hematology, Renji Hospital, School of Medicine, Shanghai Jiao Tong University, 160 Pujian Road, Shanghai, 200127, China.

\*\* Corresponding author. Department of Hematology, Renji Hospital, School of Medicine, Shanghai Jiao Tong University, 160 Pujian Road, Shanghai, 200127, China. Department of Hematology, Punan Hospital, Pudong New District, Shanghai, 200011, China.

E-mail addresses: [dujun@renji.com](mailto:dujun@renji.com) (J. Du), [houjian@medmail.com.cn](mailto:houjian@medmail.com.cn) (J. Hou).

<sup>1</sup> These authors contributed equally to this work.

<https://doi.org/10.1016/j.heliyon.2024.e30123>

Received 11 April 2024; Accepted 19 April 2024

Available online 20 April 2024

2405-8440/© 2024 Published by Elsevier Ltd.

This is an open access article under the CC BY-NC-ND license

(<http://creativecommons.org/licenses/by-nc-nd/4.0/>).

## 1. Introduction

MM is the second most common hematologic malignancy. Over the last 30 years, MM's worldwide incidence and mortality rates have more than doubled [1]. According to data from the Global Burden of Disease (GBD), there were approximately 156,000 incident cases, 113,000 deaths, and 2.50 million Disability-Adjusted Life Years (DALYs) due to MM globally in 2019.

MM exhibits significant biological and clinical heterogeneity, and precise stratification and subtyping are essential for disease diagnosis and treatment [2]. The initial staging system for MM was based on tumor burden, including indicators such as hemoglobin levels, bone destruction, M protein quantity, and serum calcium, known as the Durie-Salmon staging system. However, its application has certain limitations and inadequate predictive performance for prognosis [3]. The commonly used International Staging System (ISS) is based on  $\beta$ 2-microglobulin and albumin. In 2015, the International Myeloma Working Group (IMWG) proposed the Revised International Staging System (R-ISS) by incorporating lactate dehydrogenase levels and cytogenetic factors into the traditional ISS staging. The high-risk cytogenetic factors include del(17p) and/or t(4; 14) and/or t(14; 16) [4]. The researchers refined the R-ISS by integrating additive values of risk features such as 1q+. Nonetheless, the R2-ISS model still excludes prognostically significant molecular data, like next-generation sequencing or gene-expression profiling [5]. The Mayo Stratification for Myeloma and Risk-Adapted Therapy (mSMART) is a prognostic stratification system developed by the Mayo Clinic based on the cytogenetic and molecular genetics of MM. In mSMART 3.0, MM is categorized into high-risk and standard-risk groups. High-risk MM includes del(17p), t(14; 20), t(14; 16), t(4; 14), 1q+, or p53 mutation [6]. Although staging systems have progressed from biochemical indicators to the genomic features, pivotal determinants of disease such as cellular cytogenetic abnormalities and infiltrating immune cell characterization remain underrepresented in predictive model development, hindering the elucidation of disease complexity and personalized treatment translation [7].

Cellular cytogenetic abnormalities have become MM's main criteria for risk stratification [8]. The pathogenesis of MM involves a multi-gene, multi-stage, and multi-step process characterized by genomic instability in tumor cells and evident clonal heterogeneity. Dominant clones coexist with multiple subclones, while the MM genome undergoes dynamic evolutionary processes, accumulating genetic aberrations during this progression [9]. Chromosomal defects, genetic mutations, their impact on cellular signaling pathways, and epigenetic changes in the genome may significantly contribute to the onset and progression of MM. TP53 is the fifth most common mutations (8 %) in MM patients [10]. TP53, located at 17p13.1, is a critical gene associated with adverse prognosis in MM [11]. P53 primarily induces cell cycle arrest and apoptosis by transcribing P21 in response to DNA damage. Moreover, it governs various other biological processes, such as proliferation, metabolism, inflammation, and autophagy [12]. Previous studies identified TP53, MDM2, and others as critical genes involved in the development and progression of MM. Furthermore, the dysregulation of p53 signaling pathway might associate with MM pathogenesis [13,14]. These findings demonstrate the crucial role of TP53 in MM and suggest the immense value of investigating the p53 signaling pathway.

The disease progression is also significantly influenced by the immunosuppressive microenvironment generated by cellular and non-cellular components within the bone marrow (BM) niche. Research has shown that immune-infiltrating cells, such as mast cells, T cells, macrophages, dendritic cells, and neutrophils, create an immunosuppressive microenvironment that facilitates immune evasion of MM cells and promotes tumor progression [15–17]. Moreover, an altered immune surveillance is a prominent feature of MM, involving the abnormal overexpression of crucial immune checkpoint molecules such as cytotoxic T-lymphocyte-associated protein 4 (CTLA-4) and PD-1/PD-L1 [18]. These pathways play a crucial role in immune homeostasis by preserving immune tolerance, regulating the magnitude and duration of immune responses, and preventing harm to healthy tissues [19,20].

Immunotherapy has demonstrated excellent efficacy in MM [21]. Targeting the molecular interactions between MM plasma cells and the BM microenvironment to restore immune system homeostasis represents an ideal therapeutic approach. Preclinical models that reflect MM's genetic and immunological characteristics have been established; nonetheless, their integration into clinical prognostic systems is insufficient [22]. Consequently, we aim to establish a novel prognostic model for MM by combining both aspects to optimize prognostic stratification and treatment for MM patients.

## 2. Methods

### 2.1. Data source

The training cohort consisted of 776 MM patients from the MMRF CoMMpass study, encompassing both gene datasets and clinical information. A detailed overview of the training cohort can be found in Table S1. GSE136337 with 215 samples was enrolled as the validation set. A comprehensive summary of the validation cohort is summarized in Table S2.

### 2.2. Quantification and identification of p53-related genes and TIC cells

We extracted 68 genes that make up the p53 signaling pathway from the KEGG database (pathway "hsa04115"). The hazard ratios (HR) and 95 % confidence intervals (CI) for all genes were obtained using univariate Cox regression analysis. Among them, 25 genes were selected based on the Wald test with p-value <0.05 and HR > 1.5. To address issues of collinearity and overfitting, we further refined the model using the LASSO method. The LASSO coefficient profiles (Figure S2A) and the selection of the tuning parameter ( $\lambda$ ) through 10-fold cross-validation (Figure S2B) were critical in determining the final inclusion of 16 significant p53-associated genes. To evaluate infiltrating immune cell characterization of MM, we used gene expression profiles to estimate fractions of 22 immune cells

through the CIBERSORT algorithm, known for its accuracy in quantifying specific cell subsets like blood [23].

### 2.3. Establishment of p53 score, TIC score, and p53-TIC classifier

We calculated the coefficients and HR by multivariable Cox regression analysis for the 15 p53-related genes and the six immune cells in the final model. To address the impact of skewed distributions and enhance the stability of the parameters, we utilized bootstrap resampling with 1000 iterations to estimate the standard errors (SE).  $A_i$  or  $A_j$  are each tumor sample's gene or TIC cell abundances. The final score was determined using the following formula.

$$\text{p53 score} = \sum_{i=1}^{15} \frac{\ln(\text{HR}_i)}{\text{SE}_i} * A_i$$

$$\text{TIC score} = \sum_{j=1}^6 \frac{\ln(\text{HR}_j)}{\text{SE}_j} * A_j$$

Subsequently, the p53 and TIC scores were combined to create the p53-TIC classifier. The patients were then categorized into four subgroups using the mean values of the p53 score and TIC score and  $\text{p53}^{\text{high}}/\text{TIC}^{\text{high}}$ ,  $\text{p53}^{\text{high}}/\text{TIC}^{\text{low}}$ ,  $\text{p53}^{\text{low}}/\text{TIC}^{\text{high}}$ , and  $\text{p53}^{\text{low}}/\text{TIC}^{\text{low}}$ .

### 2.4. Biological enrichment analysis

The WGCNA enrichment analysis was utilized to identify modules of highly correlated genes in four subgroups. This analysis allowed for the exploration of gene modules associated with specific traits or conditions, facilitating the discovery of potential biomarkers or therapeutic targets [24].

Gene Set Enrichment Analysis (GSEA) and Gene Ontology (GO) analysis were performed by the “clusterProfiler” package in R. Metascape (<http://metascape.org>) was utilized to conduct KEGG pathway analysis.

### 2.5. TIDE and proteomaps

After observing significant differences in the expression of specific immune checkpoints among subgroups, we employed Tumor Immune Dysfunction and Exclusion (TIDE) to predict the response to immune therapy ([tide.dfci.harvard.edu](http://tide.dfci.harvard.edu)). This algorithm is built upon the signatures of T-cell dysfunction and exclusion to predict the response of patients to immune checkpoint blockade (ICB) therapy. TIDE scoring offers a superior assessment of the efficacy of anti-PD1 and anti-CTLA4 treatments compared to commonly used biomarkers in clinical settings, such as TMB, PD-L1 levels, and interferon [25]. We further depicted the quantitative composition of proteins, focusing on protein function based on the KEGG Pathways gene classification using a web tool (<https://www.proteomaps.net>).

### 2.6. Statistical analysis

The statistical analysis was conducted using R 4.2.2., incorporating standard tests, Spearman correlation, log-rank test, and Cox proportional hazard regression. The association between the p53 and TIC scores was assessed using the Spearman correlation method. The Cox proportional hazard regression and log-rank test were employed to investigate potential independent predictors of patients' prognosis. The significance threshold of P-values is 0.05.

## 3. Results

### 3.1. Construction of the model

The schematic diagram of the entire study is shown in Fig. 1. A total of 776 samples from MMRF were included to construct the integrated model. We extracted the expression levels of 68 genes from the p53 signaling pathway and 22 infiltrating immune cells through CIBERSORT (Fig. 2A–S1). Specific p53-associated genes and immune cells were selected based on statistical significance and clinical relevance. To screen p53-related genes, we initially employed univariate Cox regression analysis to identify 25 genes as independent prognostic factors ( $\text{HR} > 1.5$ ,  $p < 0.01$ ). Subsequently, we employed LASSO regression for variable selection and regularization, resulting in the final selection of 15 genes (Figure S2). This step was crucial to prevent overfitting and enhance the model's generalization ability. The relationship between certain genes included in the model and the pathogenesis and progression of MM has been explored in previous studies [26–28].

Regarding infiltrating immune cell characterization, we utilized Kaplan-Meier survival analysis to identify six immune cell types that demonstrate significant protective value ( $p < 0.05$ ) and hold clinical significance based on the infiltration abundance, namely Mast cells activated, T cells CD4 memory resting, Neutrophils, T cells CD4 memory activated, Monocytes, and NK cells activated (Figure S4). The dysregulation of these immune cells may constitute a significant factor in the promotion of MM, and concurrently, may serve as potential therapeutic targets for its treatment [29–32]. Fig. 2B illustrates the relationship between the included genes and

the cellular expression levels. Positive correlations were observed among p53-related genes, while the associations between genes and cells exhibited relatively weak correlations.

Subsequently, the p53 score and TIC score were developed using multivariate Cox regression optimized with the bootstrap algorithm. The samples were divided into high and low groups based on the median values of the p53 score and TIC score. Patients in p53<sup>low</sup>/TIC<sup>high</sup> group exhibited significantly prolonged survival in comparison to those in p53<sup>high</sup>/TIC<sup>low</sup> group (Fig. 2C and D). The p53<sup>high</sup> group was significantly enriched in DNA replication, mismatch repair, and proteasome pathways (Fig. 2E). On the other hand, the TIC<sup>low</sup> group showed significant enrichment in allograft rejection, asthma, and graft versus host disease pathways (Fig. 2F).

Based on the results, we further considered combining the two scores to obtain a more prognostically valuable p53-TIC classifier. The samples were divided into four subgroups: p53<sup>low</sup>/TIC<sup>high</sup>, p53<sup>low</sup>/TIC<sup>low</sup>, p53<sup>high</sup>/TIC<sup>low</sup> and p53<sup>high</sup>/TIC<sup>high</sup>. Patients in the p53<sup>high</sup>/TIC<sup>low</sup> subgroup exhibited the worst prognosis among the four subgroups (Fig. 2G). Patients in the p53<sup>low</sup>/TIC<sup>low</sup> and p53<sup>high</sup>/TIC<sup>high</sup> subgroups displayed a similar prognosis. Therefore, these two subgroups were combined into a mixed subgroup (Fig S7). The model's predictive performance was evaluated using time-ROC analysis, and the results indicated that the classifier had the best predictive performance for three-year survival (AUC = 0.80) (Fig. 2H).

### 3.2. Biological enrichment analysis among different p53-TIC subgroups

Given the significant prognostic disparities discerned the p53-TIC classifier, we performed a cellular signaling pathway analysis on the p53-TIC subgroups. The subgroups exhibited distinct patterns regarding the expression of genes associated with tumor proliferation and cancer metabolism (Fig. 3A). The WGCNA co-expression network was constructed with 776 samples and 5000 genes, and a network with five co-expression modules was identified (Fig. 2B). Except for the gray module, which contained uncategorized genes, nearly all modules correlated significantly with four subgroups. Interestingly, brown and yellow modules showed opposite correlations with the p53<sup>high</sup>/TIC<sup>low</sup> and p53<sup>low</sup>/TIC<sup>high</sup> subgroups. The brown and yellow modules positively related with the p53<sup>high</sup>/TIC<sup>low</sup> subgroup but showed a negative relation with the p53<sup>low</sup>/TIC<sup>high</sup> subgroup (Fig. 3C–S10). This finding suggested a potential association between these gene modules and prognostic outcomes.

The brown module exhibited significant enrichment in gene ontology (GO) categories related to chromatin organization, protein deubiquitylation, and epigenetic regulation of gene expression (Fig. 3D). The yellow module genes, on the other hand, were highly associated with immune functions such as response to the bacterium, innate immune response, defense response to the bacterium, humoral immune response, and antimicrobial humoral response, indicating a robust anti-tumor immune response in patients belonging to the TIC<sup>low</sup> subgroup (Fig. 3E). This observation aligned with the higher expression levels of immune cells in the TIC<sup>low</sup> subgroup, potentially contributing to immune resistance, which could be linked to the diminished survival outcomes observed in the

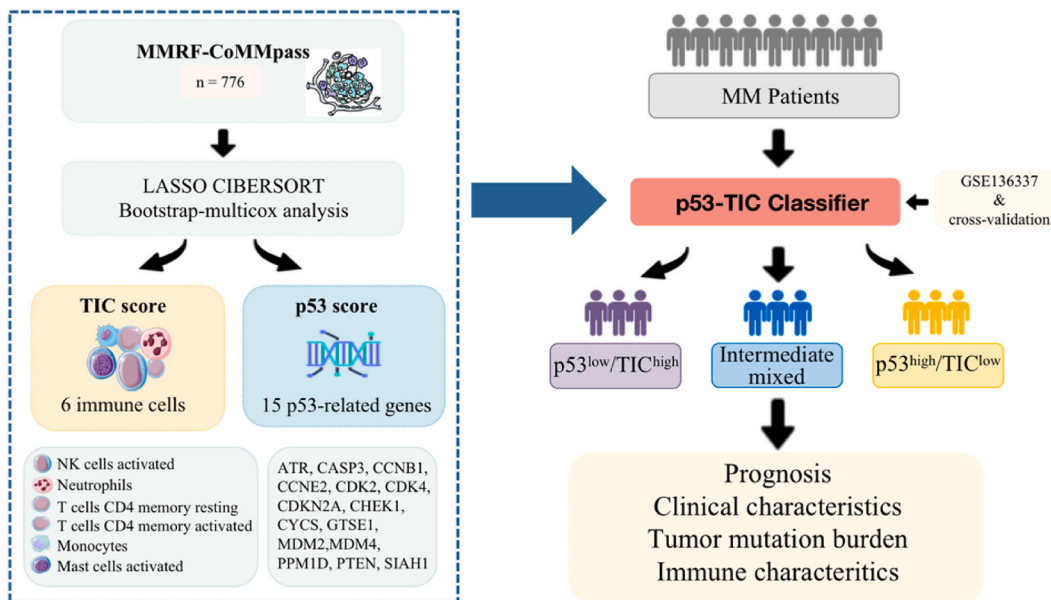
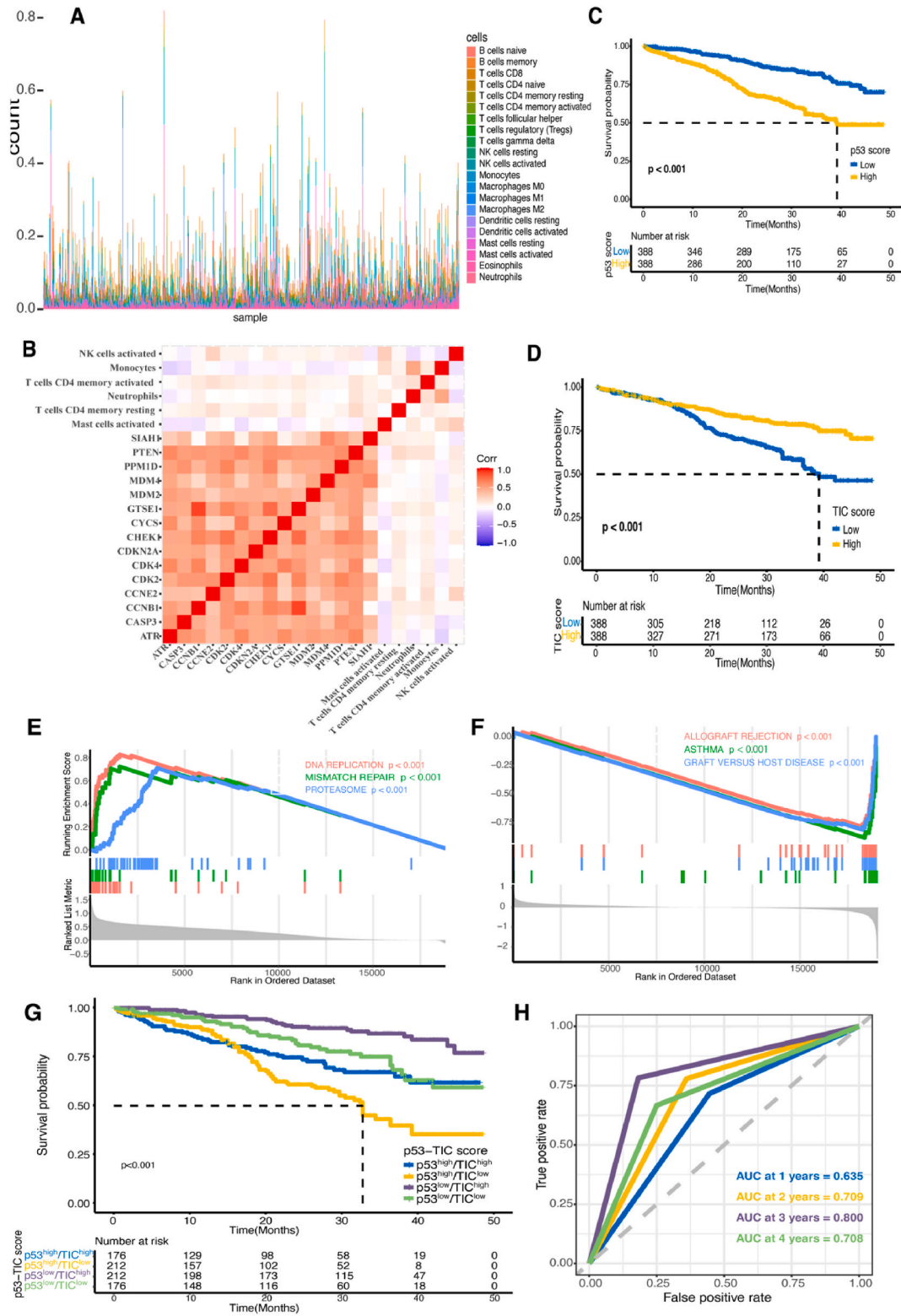


**Fig. 1.** The schematic diagram of the entire study. A total of 776 samples were included from The MMRF CoMMPass database. Using univariate regression analysis and the Lasso algorithm applied to the KEGG p53 signaling pathway gene set, 15 significant p53-associated genes were identified. Additionally, the CIBERSORT algorithm was employed to analyze the TIC, uncovering six immune cell types with autonomous prognostic risk factors identified through univariate regression analysis. Subsequently, TIC and p53 scores were derived using the bootstrap-multicox method. Utilizing the composite score, we developed a p53-TIC classifier and validated the robustness and generalization capacity through external validation on the GSE136337 dataset (n = 215) and internal ten-fold cross-validation on the MMRF CoMMPass dataset. Furthermore, subgroup analysis explored prognosis, clinical characteristics, tumor mutation burden, and immune traits.



(caption on next page)

**Fig. 2.** Establishment of Screening and Prediction Models for p53-related genes and TIC Cells. (A) Results of tumor immune infiltration based on the CIBERSORT Algorithm, illustrating the proportions of 21 infiltrating immune cell types in 776 samples, excluding plasma cells. (B) Correlations among 15 p53-related genes and 6 TIC cells. (C) Kaplan-Meier survival curves with p53 score. (D) Kaplan-Meier survival curves with TIC score. (E) GSEA results of the three most significantly correlated signaling pathways with the p53 score: DNA replication, mismatch repair, and proteasome pathways. (F) GSEA results of the three most significantly correlated signaling pathways with the TIC score: allograft rejection, asthma, and graft versus host disease. (G) Kaplan-Meier overall survival curves ( $n = 776$ ) classified into four subgroups according to the p53-TIC classifier ( $p53^{\text{low}}/\text{TIC}^{\text{high}}$ ,  $p53^{\text{low}}/\text{TIC}^{\text{low}}$ ,  $p53^{\text{high}}/\text{TIC}^{\text{high}}$  and  $p53^{\text{high}}/\text{TIC}^{\text{low}}$ ). (H) The nomogram showing the survival probability at 1-, 2-, 3-, and 4-year based on the p53-TIC classifier.  $p < 0.05$  means it is statistically significant.

$\text{TIC}^{\text{low}}$  group.

Moreover, proteomaps were constructed to visually depict the characteristics of protein functional enrichment for differentially expressed genes in  $p53^{\text{high}}/\text{TIC}^{\text{low}}$  and  $p53^{\text{low}}/\text{TIC}^{\text{high}}$  subgroups. Upregulated genes in the  $p53^{\text{high}}/\text{TIC}^{\text{low}}$  subgroup compared to  $p53^{\text{low}}/\text{TIC}^{\text{high}}$  exhibited more significant enrichment in transcription, signal transduction, biosynthesis, and the immune system, which are pivotal in mediating the anti-tumor efficacy and regulating the physiological functions of cells (Fig. 5G). These findings suggested that the integrated signatures of the p53 signaling pathway and TIC may aid in understanding the tumor biology underlying the observed prognostic distinctions.

### 3.3. Clinical characteristics and validation

In order to comprehensively assess the prognostic significance of the p53-TIC classifier, we conducted univariate and multivariate Cox regression analyses on the cohorts (Fig. 4A and B). The p53-TIC classifier was significantly associated with overall survival and demonstrated a statistically significant prognostic value. In the multivariate Cox regression analysis, the HR for the p53-TIC classifier was 2.0, indicating a superior prognostic value compared to the ISS stage. Moreover, the p53-TIC classifier displayed robust prognostic predictive performance in subgroups delineated by age, stage, and gender, underscoring the classifier's remarkable consistency (Fig. 4C-H).

We further stratified patients in the three ISS stages by integrating the p53-TIC classifier with the MM tumor stage. Notably, survival outcomes among advanced-stage MM patients with  $p53^{\text{high}}/\text{TIC}^{\text{low}}$  differed significantly from those in the advanced-stage  $p53^{\text{low}}/\text{TIC}^{\text{high}}$  cohort. This suggested that synergistic integration of the p53-TIC classifier and ISS stage enhances the predictive accuracy beyond that achievable with the ISS staging alone (Figure S11).

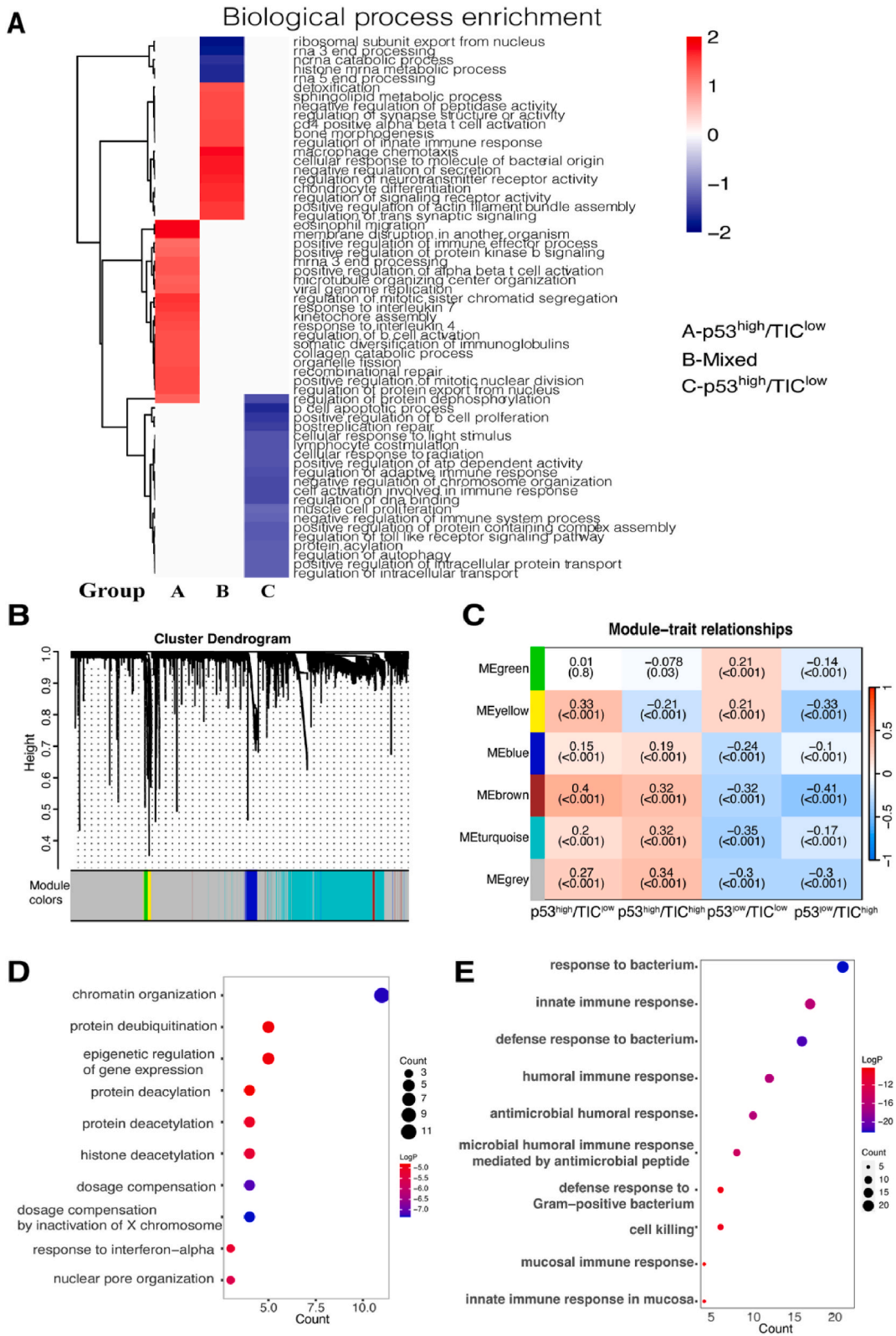
To validate the stability and generalization ability of the model, we conducted dual validation through both external and internal approaches. The external validation of the model was facilitated through the GSE136337 dataset, with 215 specimens accompanied by comprehensive clinical data. The survival curves indicated that p53-TIC staging model had great prognosis value and the  $p53^{\text{high}}/\text{TIC}^{\text{low}}$  group had the poorest prognosis (Figure S12). Furthermore, we employed internal ten-fold cross-validation, and the selected 15 genes and six immune cells were retained. We recalculated the score for each fold and constructed a prognostic model using the training set. Subsequently, we evaluated the performance of the model in the validation set (Figure S13). The average AUC of 1–4 years was 0.66, 0.68, 0.77, and 0.73, respectively. These results demonstrate the excellent stability and generalization ability of the model.

### 3.4. Immune characteristics

We proceeded to investigate the somatic alterations in tumors across p53-TIC subgroups. The  $p53^{\text{high}}/\text{TIC}^{\text{low}}$  subgroup exhibited the highest TMB, suggesting potential sensitivity to immunotherapeutic interventions (Figure S14). Nevertheless, the integration of TMB scores with the p53-TIC classifier did not enhance the precision in prognosticating more favorable patient outcomes (Figure S15).

Furthermore, we explored the top 20 variant mutations in the two subgroups with the most significant differences in prognosis. Missense mutation was the most common mutation type in both subgroups. Notably, IGHV2-70 (Immunoglobulin Heavy Variable 2–70), a protein-coding gene highly associated with antigen binding, had the highest mutation rate among the two groups. Furthermore, regarding the mutation rate, within the  $p53^{\text{high}}/\text{TIC}^{\text{low}}$  subgroup, p53 exhibited a prevalence of mutations at the eighth position (11 %), surpassing the  $p53^{\text{low}}/\text{TIC}^{\text{high}}$  group (Figure S16). Impaired tumor-suppressive function resulting from p53 mutations may be one of the contributing factors to the notably poorer prognosis observed in  $p53^{\text{high}}/\text{TIC}^{\text{low}}$  subgroup.

To explore potential immune-targeted therapies, we further investigated the expression profiles of 22 crucial immune checkpoints across subgroups. The results revealed that except for BTLA and PDCD1LG2, the expression levels of the other immune checkpoints were higher in the  $p53^{\text{high}}/\text{TIC}^{\text{low}}$  subgroup compared to the  $p53^{\text{low}}/\text{TIC}^{\text{high}}$  subgroup. Significant differences were observed for CD47, CD86, PD1, and CTLA4 (Fig. 5A–D, S17). This suggests that the  $p53^{\text{high}}/\text{TIC}^{\text{low}}$  subgroup was in a state of heightened immune suppression, which may explain the poorer prognosis observed. Consequently, overcoming immune suppression may be the key to treating such patients. Hypothesizing whether the p53-TIC classifier could serve as a predictor of clinical responses, we, therefore, assessed the p53-TIC classifier's ability to predict therapeutic responses and used TIDE to predict response rates to anti-PD1 and anti-CTLA4 immunotherapy within the subgroups. The results demonstrated that the  $p53^{\text{high}}/\text{TIC}^{\text{low}}$  subgroup had the highest response rate, reaching 40 %, surpassing the 31 % response rate observed in the  $p53^{\text{low}}/\text{TIC}^{\text{high}}$  subgroup. Furthermore, we employed the Proteomaps to uncover the mechanism behind the p53-TIC classifier's predictive capacity in ICB responses. Intriguingly, the Proteomaps configurations depicted in Fig. 5G and H showcased pronounced congruencies. This molecular congruence offers a biological rationale for potential mechanisms underlying the response to immune-based therapies.



(caption on next page)

**Fig. 3.** Bioinformatics Enrichment Analysis according to the p53-TIC classifier. (A) Fast Gene Set Enrichment Analysis (fgSEA) results of the top 20 significantly enriched pathways in the p53<sup>low</sup>/TIC<sup>high</sup>, Mixed, and p53<sup>high</sup>/TIC<sup>low</sup> subgroups. (B) Clustering dendrogram of genes with different colors representing different modules. (C) Heatmap of the correlation between module eigengenes and four subgroups. Each cell displays the correlation coefficient (above) and P value (below). (D) Biological process GO terms for genes in the brown module. (E) Biological process GO terms for genes in the yellow module. (For interpretation of the references to color in this figure legend, the reader is referred to the Web version of this article.)

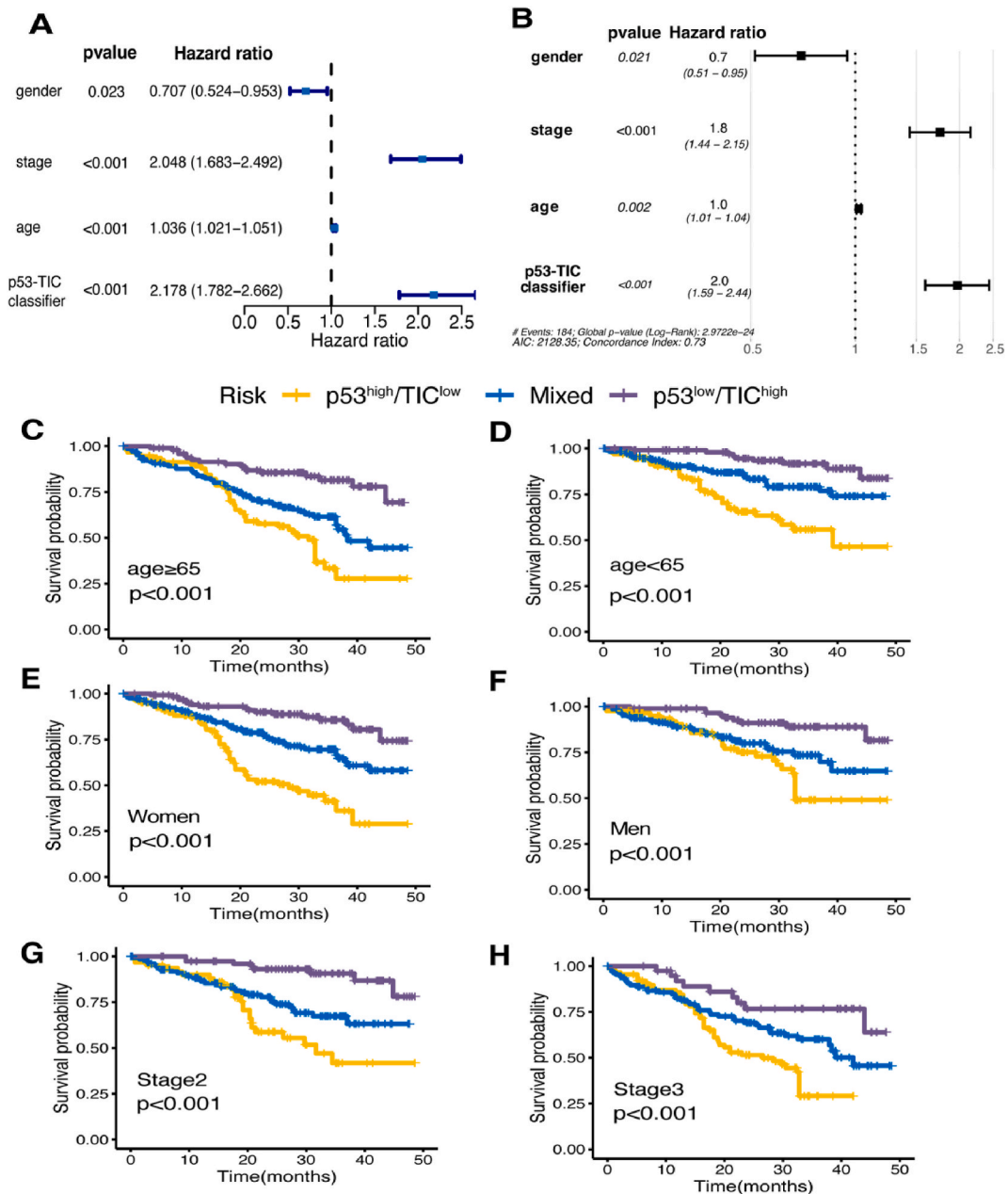


**Fig. 4.** Prognostic value of the p53-TIC classifier. (A) Univariate Cox analysis of the p53-TIC classifier. (B) Multivariate Cox analysis of the p53-TIC classifier. (C) Kaplan-Meier survival curves with patients age ≥ 65. (D) Kaplan-Meier survival curves with patients age < 65. (E) Kaplan-Meier survival curves with female patients age ≥ 65. (F) Kaplan-Meier survival curves with male patients. (G) Kaplan-Meier survival curves with patients in stage 2. (H) Kaplan-Meier survival curves with patients in stage 3. p < 0.05 means it is statistically significant.

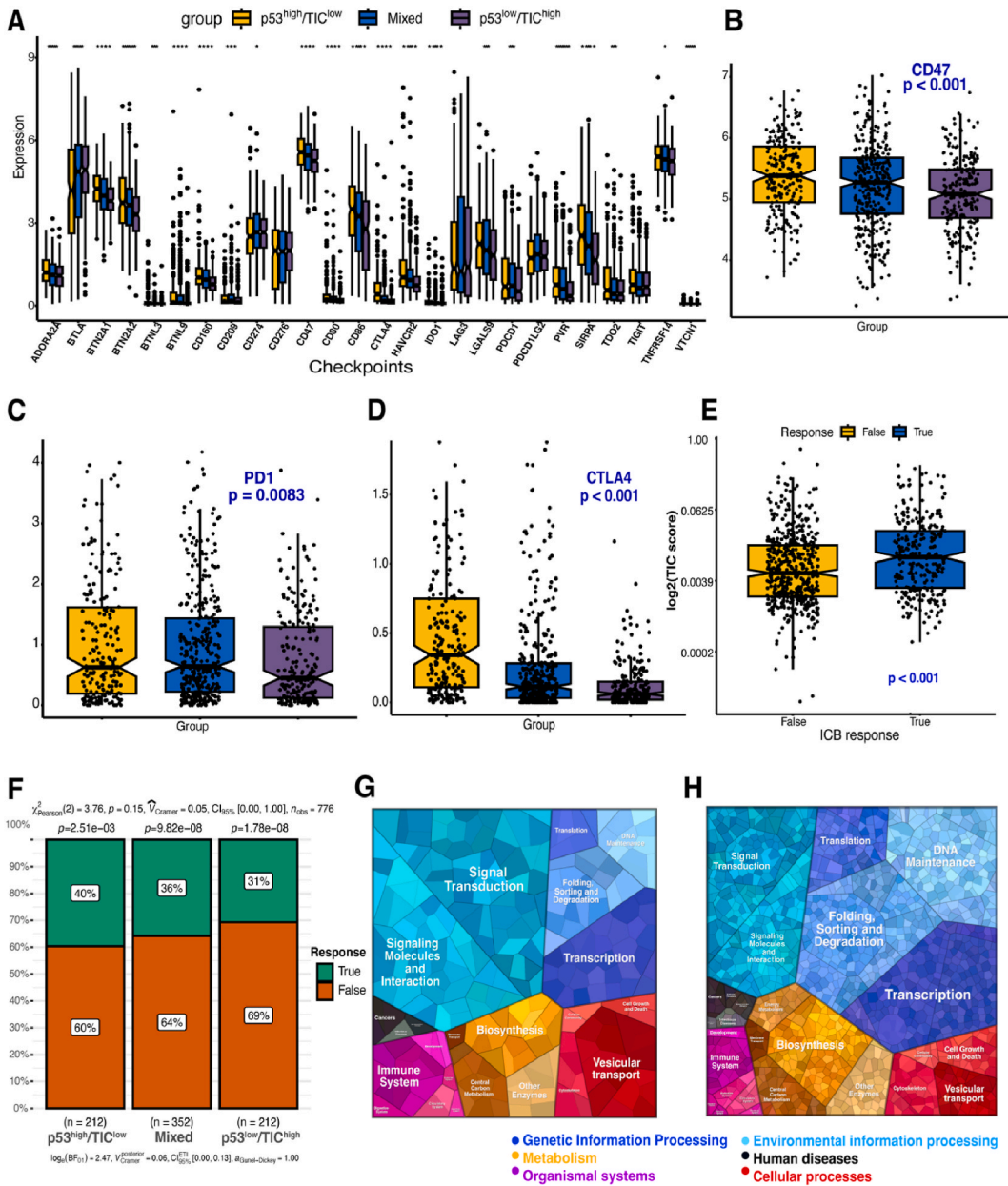


**Fig. 5.** Immune checkpoint analysis and therapy response prediction based on the p53-TIC classifier. (A) Comparison of immune checkpoints in three subgroups based on the p53-TIC classifier. (B) Expression of CD47 in three subgroups based on the p53-TIC classifier. (C) Expression of PD1 in three subgroups based on the p53-TIC classifier. (D) Expression of CTLA4 in three subgroups based on the p53-TIC classifier. (E) Comparison of TIC score in ICB response and ICB non-response subgroups. (F) Prediction of patient response to ICB using the TIDE algorithm in the  $p53^{low}/TIC^{high}$ , Mixed, and  $p53^{high}/TIC^{low}$  subgroups (TRUE, response; FALSE, non-response) (<http://tide.dfci.harvard.edu>). (G) Functional analysis plot using Proteomap for upregulated genes in the  $p53^{high}/TIC^{low}$  subgroup compared to  $p53^{low}/TIC^{high}$ . (H) Functional analysis plot using Proteomap for upregulated genes in the ICB response subgroup in comparison with the ICB non-response subgroup ([www.proteomaps.net](http://www.proteomaps.net)).

**4. Discussion**

Identifying high-risk patients upon initial diagnosis and implementing effective therapeutic strategies to improve their prognosis are challenges in diagnosing and managing multiple myeloma. Despite historical diagnostic and genomic approaches, the clinical identification of such patient cohorts still needs to be discovered, necessitating advanced techniques and refined methodologies to meet clinical demands more aptly. For instance, the ISS classifier’s assessment markers  $\beta 2$ -microglobulin can be influenced by renal dysfunction and other comorbidities, potentially muddying the interpretative clarity of these biomarkers [33]. Furthermore, most existing classifiers primarily concentrate on tumor genomic characteristics, overlooking the critical role of the immune-suppressive

microenvironment. In this study, we have developed a novel prognostic model that integrated insights into tumor molecular biology and immune-suppressive microenvironments. This model offered a more comprehensive evaluation of patient conditions, probably enabling more precise identification of high-risk groups.

In recent years, numerous studies have focused on investigating the role of p53 in MM. Del17p has been firmly established as a high-risk characteristic in MM and incorporated into the current disease staging criteria [33]. However, it is imperative to underscore that the tumor-suppressor functionality of the TP53 protein likely operates through a complex interplay of effector functions, involving intricate connections between activation triggers, cell lineage, and cellular states rather than being solely dependent on a singular pathway or transcriptional target [34]. Emerging research has unveiled potential connections between TP53 and immune checkpoint mechanisms. For instance, p53 can downregulate PD-L1 expression by inducing microRNA 34a (miR34a) [35,36]. The convergence of p53 biology with immunotherapy promises to revolutionize the future design of p53-based cancer treatments [37]. Consequently, considering the multifaceted and intricate nature of the TP53 response, we propose a creative approach that involves evaluating the enrichment of the p53 signaling pathway coupled with an analysis of immune infiltration. This innovative strategy has the potential to offer novel perspectives for MM stratification [38].

Based on the p53-TIC classifier, we identified a high-risk subgroup characterized as p53<sup>high</sup>/TIC<sup>low</sup>. This subgroup exhibited compromised DNA repair and tumor-suppressive functions within an immunosuppressive microenvironment. After identifying high-risk cohorts, discovering the optimal therapeutic regimen tailored to this group constitutes another formidable challenge. The treatment landscape for MM is undergoing a paradigm shift towards risk stratification and molecularly-driven mitigation strategies [39]. Studies have indicated that within the context of MM, disrupted immune monitoring and facilitated tumor evasion would lead to the deactivation of T-cells due to their interaction with antigens presented by malignant cells. This phenomenon leads to the inactivation of T-cells upon engagement with antigens displayed by malignant cells [20]. Building upon this physiological foundation, targeting immune checkpoints is a promising therapeutic avenue [40]. Notably, patients in the p53<sup>high</sup>/TIC<sup>low</sup> subgroup displayed elevated CD47, CTLA4, PD1, and CD86 expression levels, suggesting a potentially heightened responsiveness to immune-based therapies. This conjecture finds support in TIDE predictions. Furthermore, in conjunction with the proteomic mapping results, the enriched functionalities of the upregulated genes observed in the p53<sup>high</sup>/TIC<sup>low</sup> subgroup, as compared to the p53<sup>low</sup>/TIC<sup>high</sup> subgroup, bear a striking resemblance to those of the upregulated genes identified in the ICB response subgroup relative to the ICB non-response subgroup. These findings indicated that the pretreatment p53-TIC signature holds the potential to characterize the tumor immune microenvironment, aiding in the precise anticipation of treatment outcomes for patients. Nonetheless, it is imperative to acknowledge that the immune response predictions inferred from TIDE were not substantially elevated, intimating a potential resistance of MM to anti-PD1 and anti-CTLA4 therapies. Further research is necessary to elucidate the intricate relationship profoundly and investigate the effectiveness of alternative immunotherapeutic strategies, such as targeting CD47 and CD86 [41–43]. To conclude, the development of the p53-TIC classifier enhances prognostic stratification in MM patients and facilitates personalized treatment plans, optimizing efficacy and minimizing side effects. Additionally, it opens avenues for targeted therapeutic interventions, particularly in subgroups like p53<sup>high</sup>/TIC<sup>low</sup>. Furthermore, the classifier aids in monitoring treatment response and adjusting therapy, while also informing the design of clinical trials, thus improving their efficiency, and expediting the development of new treatments.

It is imperative to recognize that our study still possesses certain limitations. Firstly, data were exclusively sourced from retrospective public databases, which may introduce biases and may not fully encapsulate the complexities of clinical settings. Furthermore, the validation of our classifier relied on ten-fold cross-validation internally and external validation using the GSE136337 dataset, suggesting that further validation through broader clinical cohorts is warranted for a more comprehensive evaluation. Moreover, due to constraints related to the original dataset, a direct comparison of our model with the latest model was not feasible. We aim to address this limitation in future research by incorporating data from our clinical cohorts, which will allow for a more thorough comparison and potential integration with established models such as the R2-ISS. Lastly, the identified p53-TIC signatures based on gene expression require further experimental validation to confirm their biological relevance.

In conclusion, integrating p53-associated genes and infiltrating immune cell characterization holds promise for augmenting the prediction of prognosis and therapy responses.

### Availability of data

All data in the main text or supplemental material are available. The genomic and clinical data supporting the findings of this study are available from the UCSC Xena database (MMRF CoMMpass study) and NCBI GEO under the accession number GSE136337.

### Funding

This study was supported by Shanghai Shenkang Hospital Development Center of China (No. SHDC2020CR2070B).

### Ethics approval and consent to participate

None.

### Consent for publication

All authors reviewed and approved the final manuscript.

## CRediT authorship contribution statement

**Jun-Ting Lv:** Writing – review & editing, Writing – original draft, Project administration, Methodology, Formal analysis. **Yu-Tian Jiao:** Writing – review & editing, Writing – original draft, Validation, Methodology, Investigation, Formal analysis. **Xin-Le Han:** Writing – review & editing, Writing – original draft, Validation, Project administration, Methodology, Formal analysis. **Yang-Jia Cao:** Visualization, Writing – original draft, Methodology, Investigation, Formal analysis. **Xu-Kun Lv:** Visualization, Project administration, Investigation, Formal analysis. **Jun Du:** Writing – review & editing, Supervision, Resources, Methodology, Funding acquisition. **Jian Hou:** Writing – review & editing, Supervision, Resources, Methodology, Funding acquisition.

## Declaration of competing interest

The authors declare that they have no known competing financial interests or personal relationships that could have appeared to influence the work reported in this paper.

## Acknowledgement

None.

## Appendix A. Supplementary data

Supplementary data to this article can be found online at <https://doi.org/10.1016/j.heliyon.2024.e30123>.

## References

- [1] L.H. Zhou, et al., Measuring the global, regional, and national burden of multiple myeloma from 1990 to 2019, *BMC Cancer* 21 (1) (2021).
- [2] S.V. Rajkumar, S. Kumar, Multiple myeloma: diagnosis and treatment, *Mayo Clin. Proc.* 91 (1) (2016) 101–119.
- [3] K. Fechtner, et al., Staging Monoclonal plasma cell disease: comparison of the Durie-Salmon and the Durie-Salmon PLUS staging systems, *Radiology* 257 (1) (2010) 195–204.
- [4] A. Palumbo, et al., Revised international staging system for multiple myeloma: a report from international myeloma working group, *J. Clin. Oncol.* 33 (26) (2015) 2863–+.
- [5] Second Revision of the International Staging System (R2-ISS) for Overall Survival in Multiple Myeloma: A European Myeloma Network (EMN) Report within the HARMONY Project.
- [6] S.V. Rajkumar, Multiple myeloma: 2020 update on diagnosis, risk-stratification and management, *Am. J. Hematol.* 95 (5) (2020) 548–567.
- [7] P. Hagen, J. Zhang, K. Barton, High-risk disease in newly diagnosed multiple myeloma: beyond the R-ISS and IMWG definitions, *Blood Cancer J.* 12 (5) (2022) 83.
- [8] S.K. Kumar, S.V. Rajkumar, The multiple myelomas - current concepts in cytogenetic classification and therapy, *Nat. Rev. Clin. Oncol.* 15 (7) (2018) 409–421.
- [9] S.K. Kumar, et al., Multiple myeloma, *Nat. Rev. Dis. Prim.* 3 (2017).
- [10] B.A. Walker, et al., Mutational spectrum, copy number changes, and outcome: results of a sequencing study of patients with newly diagnosed myeloma, *J. Clin. Oncol.* 33 (33) (2015) 3911–+.
- [11] C.J. Neuse, et al., Genome instability in multiple myeloma, *Leukemia* 34 (11) (2020) 2887–2897.
- [12] Y. Liu, W. Gu, The complexity of p53-mediated metabolic regulation in tumor suppression, *Semin. Cancer Biol.* 85 (2022) 4–32.
- [13] E. Flynt, et al., Prognosis, biology, and targeting of TP53 dysregulation in multiple myeloma, *Cells* 9 (2) (2020).
- [14] A.M. Yehia, et al., Decoding the role of miRNAs in multiple myeloma pathogenesis: a focus on signaling pathways, *Pathol. Res. Pract.* (2023) 248.
- [15] P. Leone, et al., Actors on the scene: immune cells in the myeloma niche, *Front. Oncol.* 10 (2020).
- [16] R. Vyzoukaki, et al., The impact of mast cell density on the progression of bone disease in multiple myeloma patients, *Int. Arch. Allergy Immunol.* 168 (4) (2015) 263–268.
- [17] A. Garcia-Ortiz, et al., The role of tumor microenvironment in multiple myeloma development and progression, *Cancers* 13 (2) (2021).
- [18] A.K. de Nalecz, et al., Inappropriate expression of PD-1 and CTLA-4 checkpoints in myeloma patients is more pronounced at diagnosis: implications for time to progression and response to therapeutic checkpoint inhibitors, *Int. J. Mol. Sci.* 24 (6) (2023).
- [19] T.F. Gajewski, H. Schreiber, Y.-X. Fu, Innate and adaptive immune cells in the tumor microenvironment, *Nat. Immunol.* 14 (10) (2013) 1014–1022.
- [20] S. Caserta, et al., Immune checkpoint inhibitors in multiple myeloma: a review of the literature, *Pathol. Res. Pract.* 216 (10) (2020).
- [21] A.J. Cowan, et al., Diagnosis and management of multiple myeloma A review, *JAMA, J. Am. Med. Assoc.* 327 (5) (2022) 464–477.
- [22] M. Larrayoz, et al., Preclinical models for prediction of immunotherapy outcomes and immune evasion mechanisms in genetically heterogeneous multiple myeloma, *Nat. Med.* 29 (3) (2023) 632–645.
- [23] A.M. Newman, et al., Robust enumeration of cell subsets from tissue expression profiles, *Nat. Methods* 12 (5) (2015), 453–+.
- [24] P. Langfelder, S. Horvath, WGCNA: an R package for weighted correlation network analysis, *BMC Bioinf.* 9 (2008).
- [25] P. Jiang, et al., Signatures of T cell dysfunction and exclusion predict cancer immunotherapy response, *Nat. Med.* 24 (10) (2018) 1550–+.
- [26] B.A. Walker, et al., Mutational spectrum, copy number changes, and outcome: results of a sequencing study of patients with newly diagnosed myeloma, *J. Clin. Oncol.* 33 (33) (2015) 3911–3920.
- [27] H. Wu, et al., MIR145-3p promotes autophagy and enhances bortezomib sensitivity in multiple myeloma by targeting HDAC4, *Autophagy* 16 (4) (2020) 683–697.
- [28] E. Clavero, et al., Polymorphisms within autophagy-related genes as susceptibility biomarkers for multiple myeloma: a meta-analysis of three large cohorts and functional characterization, *Int. J. Mol. Sci.* 24 (10) (2023).
- [29] J. Krejčík, et al., Daratumumab depletes CD38+ immune regulatory cells, promotes T-cell expansion, and skews T-cell repertoire in multiple myeloma, *Blood* 128 (3) (2016) 384–394.
- [30] F. Cichocki, et al., Quadruple gene-engineered natural killer cells enable multi-antigen targeting for durable antitumor activity against multiple myeloma, *Nat. Commun.* 13 (1) (2022) 7341.
- [31] O. Venglar, et al., Natural killer cells in the malignant niche of multiple myeloma, *Front. Immunol.* 12 (2021) 816499.
- [32] W. Jing, et al., Adoptive cell therapy using PD-1(+) myeloma-reactive T cells eliminates established myeloma in mice, *J Immunother Cancer* 5 (2017) 51.

- [33] R. Ciftciler, et al., Evaluation of prognostic significance of the international staging system according to glomerular filtration rate in newly diagnosed multiple myeloma patients eligible for autologous stem cell transplantation, *Turkish Journal of Hematology* 38 (1) (2021) 33–40.
- [34] E.R. Kastenhuber, S.W. Lowe, Putting p53 in context, *Cell* 170 (6) (2017) 1062–1078.
- [35] M.A. Cortez, et al., PDL1 Regulation by p53 via miR-34, *Jnci-Journal of the National Cancer Institute* 108 (1) (2016).
- [36] X. Wang, et al., Tumor suppressor miR-34a targets PD-L1 and functions as a potential immunotherapeutic target in acute myeloid leukemia, *Cell. Signal.* 27 (3) (2015) 443–452.
- [37] L.J.H. Borrero, W.S. El-Deiry, Tumor suppressor p53: biology, signaling pathways, and therapeutic targeting, *Biochim. Biophys. Acta Rev. Canc* 1876 (1) (2021).
- [38] B.J. Aubrey, A. Strasser, G.L. Kelly, Tumor-suppressor functions of the TP53 pathway, *Cold Spring Harbor Perspectives in Medicine* 6 (5) (2016).
- [39] P. Rodriguez-Otero, B. Paiva, J.F. San-Miguel, Roadmap to cure multiple myeloma, *Cancer Treat Rev.* (2021) 100.
- [40] M. Braunstein, J. Weltz, F. Davies, A new decade: novel immunotherapies on the horizon for relapsed/refractory multiple myeloma, *Expet Rev. Hematol.* 14 (4) (2021) 377–389.
- [41] J. Sun, et al., Targeting CD47 as a novel immunotherapy for multiple myeloma, *Cancers* 12 (2) (2020).
- [42] C.M. Gavile, et al., CD86 regulates myeloma cell survival, *Blood Advances* 1 (25) (2017) 2307–2319.
- [43] T. Moser-Katz, et al., PDZ proteins SCRIB and DLG1 regulate myeloma cell surface CD86 expression, growth, and survival, *Mol. Cancer Res.* 20 (7) (2022) 1122–1136.